UCRL - 74938
PREPRINT
CONF-731009--10

31962

LAWRENCE LIVERMORE LABORATORY
University of California/Livermore, California

EXOTIC CTR FUELS: NON-THERMAL EFFECTS AND LASER FUSION APPLICATIONS*

Thomas Weaver†, George Zimmerman†† and Lowell Wood

October 30, 1973

This paper was prepared for presentation at the 1973 Annual Meeting of the American Physical Society Division of Plasma Physics, Philadelphia, PA, 31 October - 3 November 1973.

*Research performed under the auspices of the USAEC.
†Also Fannie & John Hertz Foundation Fellow, Physics Dept., UC Berkeley.
††Also with Astronomy Dept., UC Berkeley.

EXOTIC CTR FUELS: NON-THERMAL EFFECTS AND LASER FUSION APPLICATIONS*

Thomas Weaver†, George Zimmerman†† and Lowell Wood

University of California Lawrence Livermore Laboratory
Livermore, CA 94550

Introduction

In the design of controlled fusion reactor systems, virtually the only fuels considered in the past have been DT, DD, and DHe^3. All three of these "standard" fuels suffer from significant shortcomings related primarily to their copious direct or indirect production of neutrons, and secondarily, in the case of DT and DHe^3, to the necessity to breed fuel components. The attendant problems of reactor wall deterioration, neutron-activated radioactive waste disposal, and of efficiently converting neutron-borne fusion energy ($\sim$ 80% for DT) to electricity have proved quite challenging and are presently being vigorously attacked.

An alternate approach to these problems, however, is to seek what we term "exotic" fusion fuel systems that would not be subject to such difficulties. Ideally, such a fuel system would involve no neutron- or radio-nuclide-producing reactions; have cheap and inexhaustibly available reactants; output most of its energy as charged particles; and have a sufficiently high energy-generation rate to be usable in projected laser fusion or other CTR systems. We have searched the light elements for such reactions and one new and promising candidate was found in the reaction: $p + B^{11} \rightarrow 3He^4 + 8.68$ Mev (denoted below as pB^{11}). In certain modes of

*Research performed under the auspices of the USAEC.
†Also Fannie & John Hertz Foundation Fellow, Physics Dept., UC Berkeley.
††Also with Astronomy Dept., UC Berkeley.

reactor operation, this reaction appears capable of substantially satisfying all of the above criteria. Other possibly interesting fuel combinations include: pLi^6, dLi^6, pBe^9, dBe^9, pB^{10}, and pN^{15}, though these suffer from relatively low reaction rates and in some cases substantial neutron and radionuclide production.

pB^{11} Fuel System Characteristics

Clean Burn. The most salient feature of the pB^{11} fuel system is that > 99.9% of its reaction products are safe, non-radioactive helium nuclei with the remainder composed of $\lesssim$ 0.1% neutrons and 0.05% radioactive particles. The small residual contamination is caused by (α,n) and (α,p) reactions on B^{11} that occur while the fusion-produced alpha particles ($1 \lesssim E_\alpha \lesssim 4$ Mev) are slowing down in the burning plasma; and also by direct thermal (p,γ) and (p,n) reactions. The characteristics of these side reactions including their rates and contribution to reactor radioisotope inventories is detailed in Table I. The radioisotope inventories are seen to be several orders of magnitude lower for pB^{11} than those for fission and DT-fusion reactors .

Cost and Abundance. B^{11} comprises 80.22% of natural boron, and is more abundant and currently projected to be cheaper to recover than either deuterium or Li^6. One particularly large and readily accessible source of B^{11} is the mineral borax, generally found in dry lake beds.

Reaction Rate and Ignition Conditions. Figure 1 shows the density-normalized thermonuclear reaction rates ($\langle\sigma v\rangle$'s) for pB^{11} and the standard fuels. The solid $\langle\sigma v\rangle$ curve for pB^{11} is based on recent experimental measurements by Tombrello, Dwarkamath, and Lowry at Caltech and Lutz, Proctor, and Bartolini at Livermore and is believed accurate to ± 20%. The dotted curve is an older $\langle\sigma v\rangle$ calculation due to Fowler, Laughlin, and Zimmerman, used in some past pB^{11} calculations and which we now consider to be overly optimistic. It is seen that for ion temperatures above 125 kev, pB^{11} has a $\langle\sigma v\rangle$ and thus a burn rate comparable to DD and DHe^3.

Figures 2 and 3 plot the density-normalized local thermonuclear energy generation rates ($\dot{E}_{TN}/n_T^2$) and relativistically correct bremsstrahlung energy loss rates ($\dot{E}_{BREMS}/n_T^2$) for various ratios of the electron to the ion temperature, for pB^{11}, pLi^6, dLi^6, pBe^9, and the standard fuels. These graphs directly indicate the conditions under which the idealized ignition criterion for optically thin systems ($\dot{E}_{TN} > \dot{E}_{BREMS}$) is met. The indicated relative proportions of the fuel constituents have been chosen to maximize $\dot{E}_{TN} - \dot{E}_{BREMS}$. From these curves it is apparent that the high bremsstrahlung radiation loss rates characteristic of the relatively high Z exotic fuels restrict the conditions under which these fuels can be ignited. In the case of pB^{11}, the electron/ion temperature ratio must be kept below 0.24 (at T_i = 250-300 kev). For pLi^6, this maximum ratio is 0.17 (at $T_i \sim 350$ kev), while for pBe^9 it must be < 0.08 (at $T_i \sim 200$ kev). One measure of what values of T_e/T_i might be attainable is to consider the steady state case (believed typical of conditions in many proposed CTR reactors), where the heating of the electrons by the fusion-heated ions is just balanced by their cooling by bremsstrahlung. The steady state bremsstrahlung loss rates have been included in Figures 2 and 3. The $\ln \Lambda = 5$ and $\ln \Lambda = 20$ cases are typical of fusion microexplosions and mirror-machine systems, respectively, where $\ln \Lambda$ is the Coulomb logarithm, a density-dependent factor proportional to the electron-ion coupling. It is seen under steady state conditons that

DT can be readily ignited, DHe^3 moderately well ignited, DD marginally ignited, and pBe^9, pLi^6, and DLi^6 probably not ignited. pB^{11} evidently falls about 20% short of steady state ignition in the laser fusion case, and about 50% short in the magnetic-confinement case.

<u>Non-Thermal Effects</u>. There are, however, a variety of non-thermal effects that can augment the pB^{11} reaction rate or reduce plasma radiation losses and thus extend the range over which ignition can occur. These effects include:

1) An ion-ion fusion chain where at least one of the 3 alpha particles from each pB^{11} reaction upscatters a proton into the $\sim$ 0.8 barn high, 300 kev wide reaction resonance centered at a 675 kev proton energy such that it reacts before being rethermalized. In this case a diverging chain reaction, exactly analogous to the fission case would be established.

2) A weak ion-ion fusion chain that didn't diverge but still caused an augmentation of the population of the high energy tail of the ion distribution, thus increasing the reaction rate above the thermal value.

3) A depopulation of the low energy ion-coupled electrons, due to upscattering by fusion-born alpha particles, thus resulting in a lower electron temperature and less bremsstrahlung radiation loss.

A computer code (FOKN) has been developed to definitively evaluate any such non-thermal effects occurring in thermonuclear burn for arbitrary types of fuel. Making the assumption of an infinite medium, FOKN follows the energy distributions of the nuclear reactants and products in detail, calculating the low-angle Rutherford scattering processes implicitly using the Fokker-Planck approximation and calculating explicitly the large angle Coulomb and nuclear scatterings and reaction processes via a transfer matrix..

The use of this code, however, requires extensive knowledge of nuclear reaction and scattering cross-sections. Due to recent measurements, however, enough of these cross-sections are now known for the pB^{11} case to allow a tentative determination of level of non-thermal effects that can be expected. This turns out to be from 5-15% in the range of density 10^{16}-10^{26} and temperature 150-350 kev we have studied so far. Figure 4 shows a typical proton spectrum during burn, compared with a Maxwellian of equivalent energy density. Such effects are expected to be substantially larger for some of the potential fusion chains described by Jetter, Post, and McNally, but the general lack of adequate cross-sections has so far inhibited us from undertaking a quantitative study on this.

pB^{11} Burn Modes

Thus, while the residual 20% error in the pB^{11} cross-section together with the non-thermal augmentation in the burn rate might allow ignition in the optically thin steady state case, it seems more promising to try to find reactor modes where either 1) ignition is not required; 2) the T_e/T_i ratio stays below its steady state or 3) a substantial fraction of the bremsstrahlung radiation is reabsorbed in the plasma.

Sub-Ignition Operation. Operation below ignition would be potentially feasible for magnetic CTR reactors with energy recycling efficiencies exceeding 67%. Such efficiencies are perhaps attainable if direct conversion techniques for high energy x-rays can be developed; for example, a generator driven by Compton scattering which has been discussed elsewhere.

In the laser fusion reactor case, energy recycling efficiencies seem inherently in the range $\lesssim 1\%$, and consequently there seems little possibility of operating such reactors below ignition.

Non-Steady State Operation. A variety of approaches appear possible here. One is the injection of a 700 kev beam of protons into a relatively cold ($\sim$ 40 kev) B^{11} plasma, although initial FOKN calculations have so far only yielded energy multiplication factors of $\sim$ 0.15 for this mode. In general, a sparse sampling of the parameter range described above shows that the equilibration time to reach the steady state solution is generally in the range 1/3 - 1/10 of the fuel burn-up time.

Optically Thick Operation. By far the most promising mode for a pB^{11} reactor is when most or all of the bremsstrahlung photons are reabsorbed within the burning plasma. This mode of operation seems uniquely possible in inertial confinement approaches to fusion, such as laser fusion where the confinement can be made effective for neutral as well as charged particles. Without such radiation losses the intrinsically high energy generation rate per unit volume of pB^{11} is capable of driving a strong detonation shock wave through an extremely ($\sim 10^5$ g/cm^3) compressed laser fusion pellet. My colleague, Dr. Lowell Wood, the next speaker, will discuss in more detail the structure of such detonation shocks and the large energy multiplication factors derivable from them.

Table I

Reaction	Q MeV	Occurrence relative to $p + B^{11} \rightarrow 3He^4$ at 250 keV	Radioisotope inventory of 1000 MWt plant, Curies	
$p + B^{11} \rightarrow C^{12} + \gamma$	16.0	5×10^{-5}	200 (Steady state)*	97% 12 + 4 MeV γ's 3% 16 MeV γ's
$p + B^{11} \rightarrow n + C^{11}$	-2.8	1.5×10^{-5}	4×10^5 (Steady state)	Thermal neutrons, $t_{1/2}(C^{11})$=20min.
$\alpha + B^{11} \rightarrow n + N^{14}$	0.2	$\lesssim 10^{-3}$	$\lesssim 3 \times 10^5$ (Nb structural activity — short-lived)	Non-thermal generation
$\alpha + B^{11} \rightarrow p + C^{14}$	0.8	$\lesssim 10^{-4}$	$\lesssim 10^3$ (Annual production)	$1 \lesssim (E_n, E_p) \lesssim 4$ MeV $t_{1/2}(C^{14})$=6000yr.
DT Fusion Reactor	—	—	$\sim 10^8 - 10^9$ (Steady state)	
Fission reactor	—	—	$\sim 10^{10}$ (Steady state)	

*O^{15} from activation of water shielding ($t_{1/2}$ = 2 min)

THERMONUCLEAR REACTION RATES

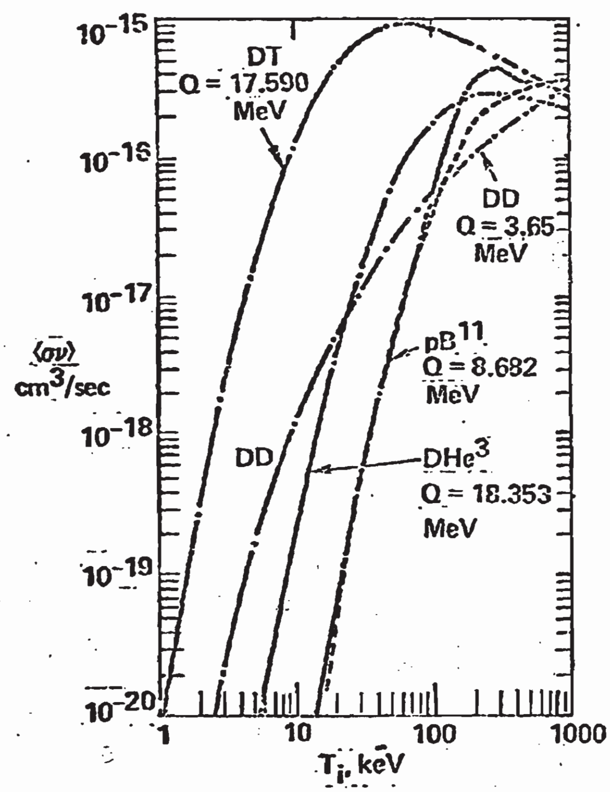

FIGURE 1

THERMONUCLEAR ENERGY GENERATION AND BREMSSTRAHLUNG LOSS RATES

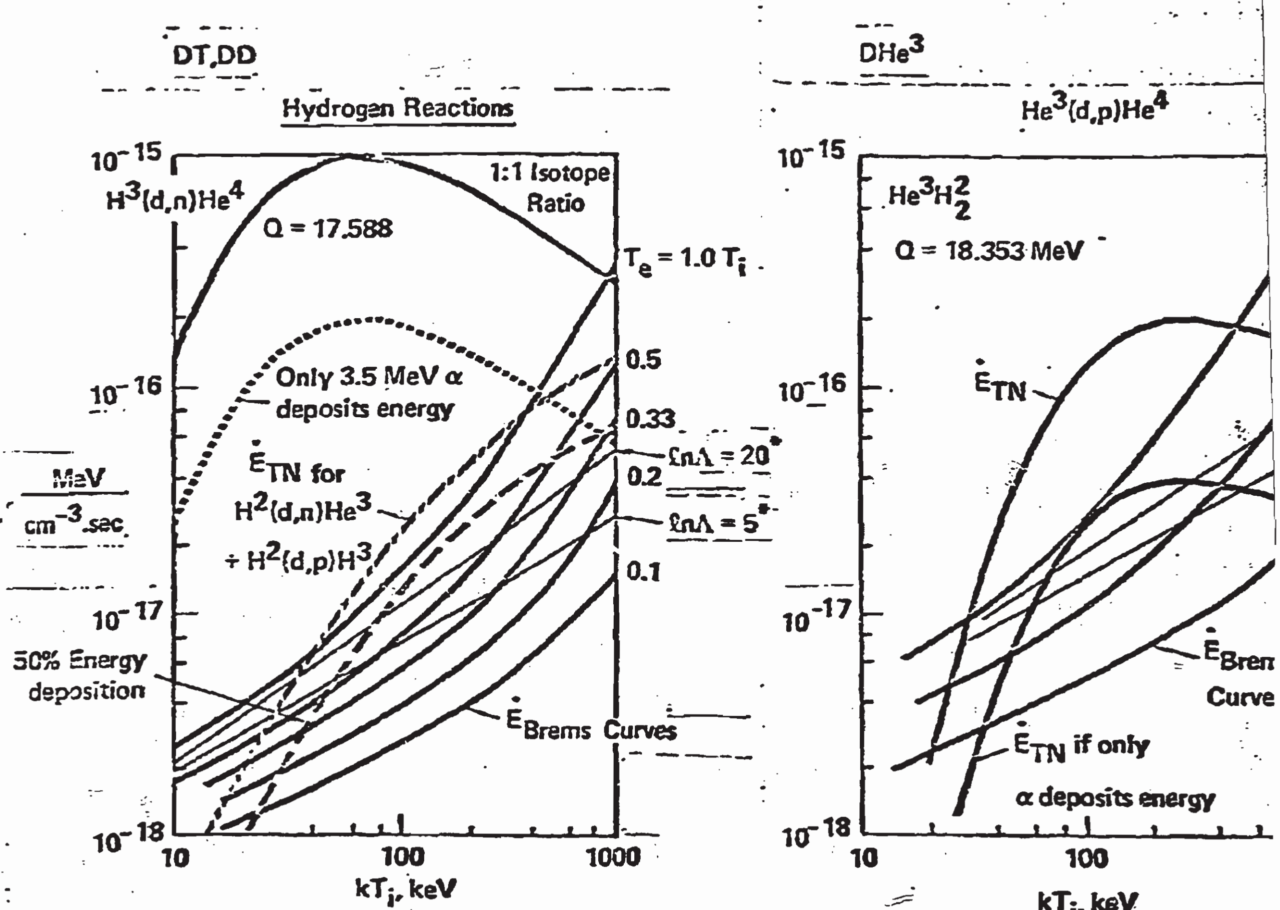

$Q_{H^2(d,n)He^3} = 3.269$ MeV

$Q_{H^2(d,p)H^3} = 4.032$ MeV

Subsequent d + t reaction not included

* $\dot{E}_{Brems}$ steady state soln.

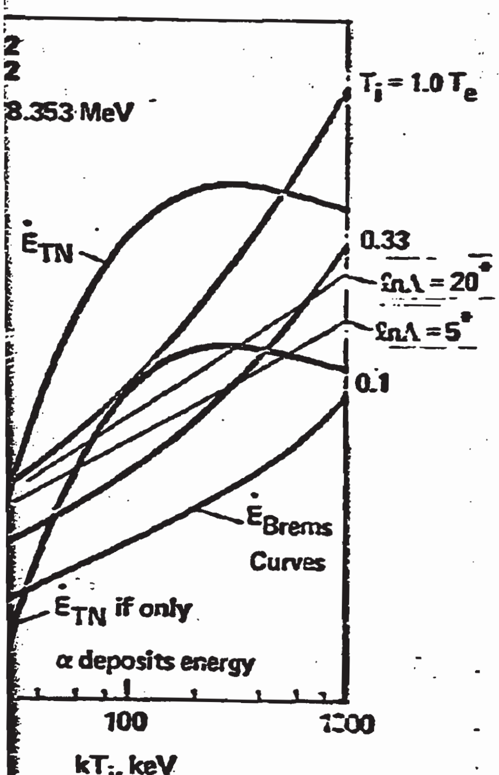

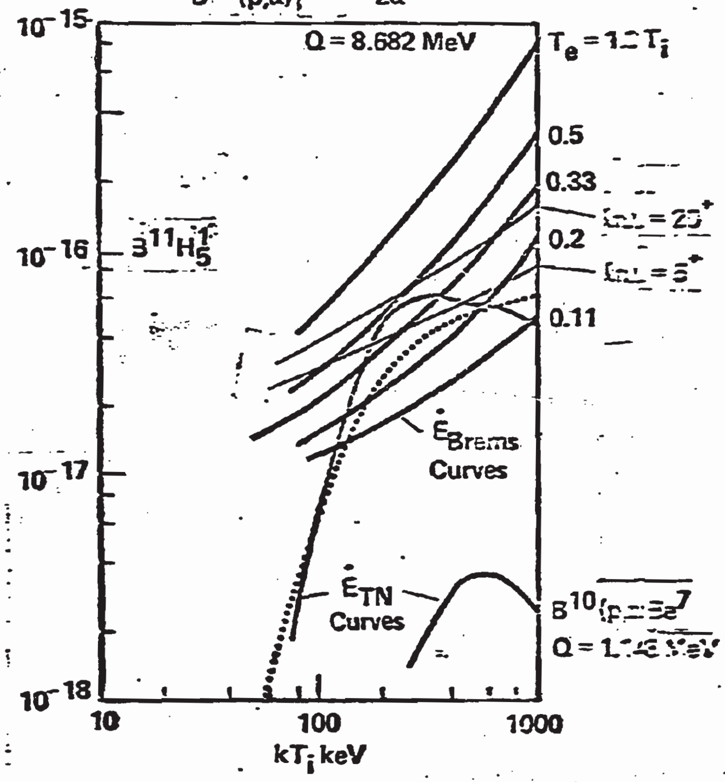

$\dot{E}_{Brems}$ steady state soln.

2

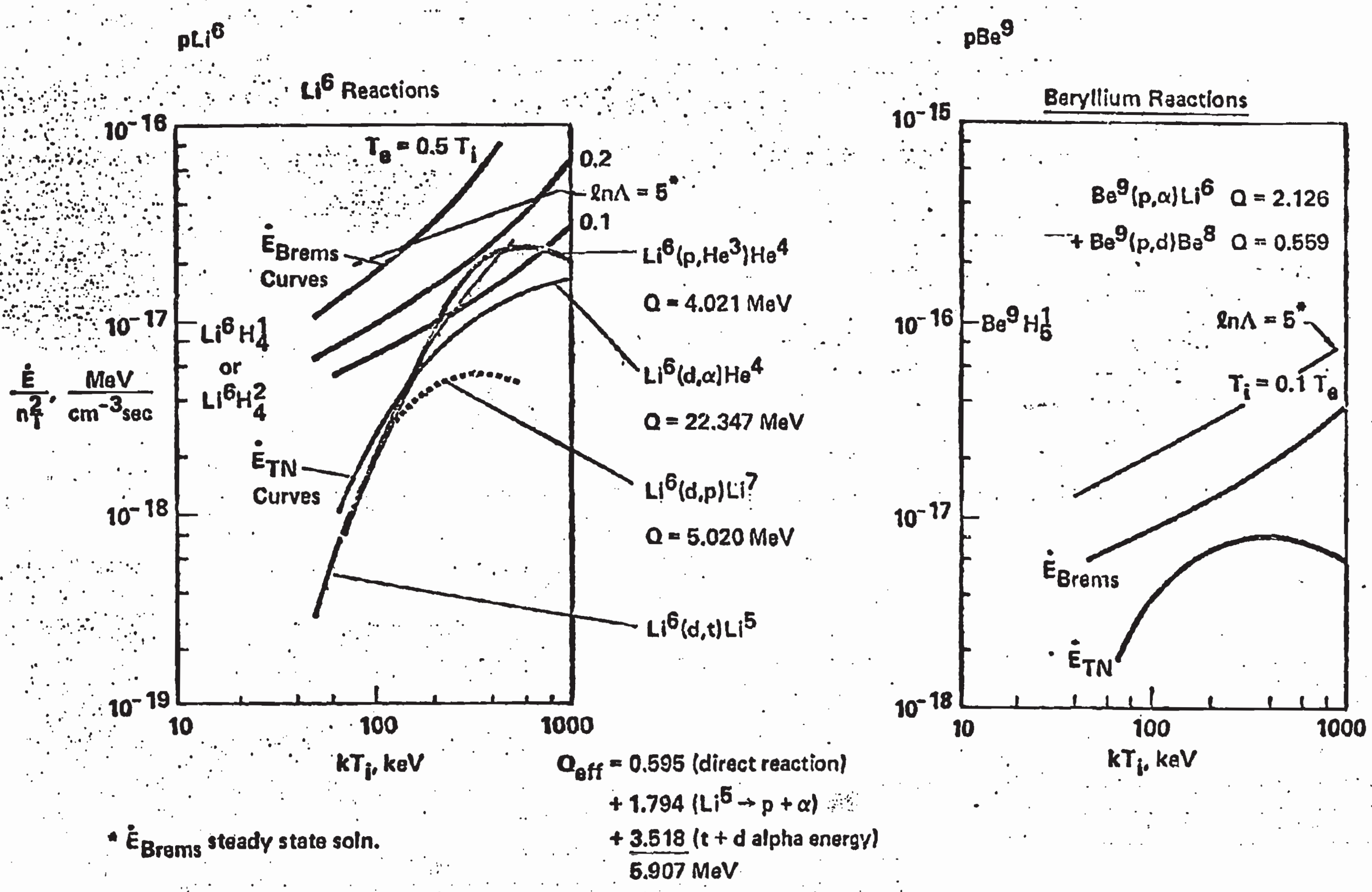

pLi6
Li6 Reactions
$\frac{\dot{E}}{n_i^2}, \frac{MeV}{cm^{-3}sec}$
10^{-16}
10^{-17}
10^{-18}
10^{-19}
10
100
1000
kT_i, keV
$T_e = 0.5 T_i$
0.2
$\ell n\Lambda = 5^*$
0.1
$\dot{E}_{Brems}$ Curves
$Li^6H^1_4$ or $Li^6H^2_4$
$\dot{E}_{TN}$ Curves
$Li^6(p,He^3)He^4$
Q = 4.021 MeV
$Li^6(d,\alpha)He^4$
Q = 22.347 MeV
$Li^6(d,p)Li^7$
Q = 5.020 MeV
$Li^6(d,t)Li^5$
Q_{eff} = 0.595 (direct reaction)
+ 1.794 ($Li^5 \rightarrow p + \alpha$)
+ 3.518 (t + d alpha energy)
5.907 MeV
* $\dot{E}_{Brems}$ steady state soln.
pBe9
Beryllium Reactions
10^{-15}
10^{-16}
10^{-17}
10^{-18}
$Be^9H^1_5$
$Be^9(p,\alpha)Li^6$ Q = 2.126
+ $Be^9(p,d)Be^8$ Q = 0.559
$\ell n\Lambda = 5^*$
$T_i = 0.1 T_e$
$\dot{E}_{Brems}$
$\dot{E}_{TN}$
10
100
1000
kT_i, keV

Figure 3

Non-Thermal Proton Spectrum

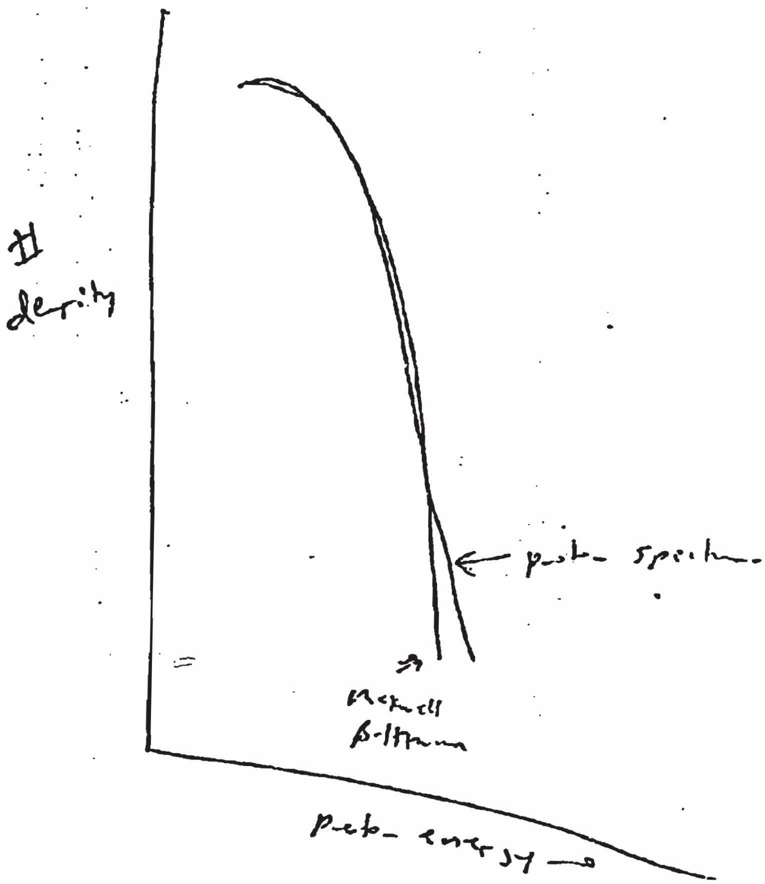

Figure 4